Red Shift for Solvatochromic Indicators as a Measure of Solvent Basicity in Polar Aprotic Media

Orland W. Kolling

Chemistry Department, Southwestern College, Winfield, Kans. 67156

The transition energies of three bathochromic dyes were determined in 15 aprotic solvent species containing N- and O-atom basic sites. Comparisons were made between the solvent-induced red shift for the dyes and various enthalpy, entropy, and free-energy functions proposed by other investigators as measures of solvent polarity. The only significant correlations occur between the transition energies and the ΔG for formation of the hydrogen-bonded adduct between the aprotic bases and p-fluorophenol.

A number of specific solvatochromic indicators have been used for the construction of empirical scales measuring the polarity of nonaqueous solvents. Among those derived from solvent-induced blue shifts, the Kosower Z values and the Dimroth-Reichardt E_T parameters have been the most successful in correlating reaction kinetics with the polarity of the solvent (1-3). The merocyanine dyes exhibit sizable bathochromic (red) shifts in their electronic spectra in less polar solvents, and these dyes have been applied to the examination of single- and two-component solvents (4, 5) and to a limited number of hydrogen-bonding systems (6-8).

Because of the excellent conformity of the red shift for phenol blue to theoretical predictions in several solvents (6, 9), it would be desirable to investigate the response of other related bathochromic indicators in a greater variety of aprotic solvents. The dyes now selected for this purpose have the structures shown in Figure 1. By contrast to the Kosower and Dimroth indicators, these three species share a common $\pi \rightarrow \pi^*$ mechanism for photon absorption in which the transition is from a weakly polar and uncharged ground state to a more strongly polar excited state. Structural analogies between the merocyanines (phenol blue and Brooker's dye VII) and nile blue A oxazone have been outlined by Davis and Hetzer (10).

In this study the transition energies (E_T) for the three solvatochromic indicators were compared to independently determined thermodynamic data for hydrogen bond donor-acceptor interactions involving N- and O-atom acceptor sites. For this purpose, the extensive tabulations of Drago et al. (11) with phenol as the reference donor and of Arnett, Mitchell, and Murty (12) using p-fluorophenol (PFP) were examined. An observed regular though nonlinear correlation between the value of E_T and the free energy of formation of the hydrogen bonded adduct in eq 1 suggests that the red shift of the indicator is a quantitative response to the Lewis basicity for polar aprotic solvents.

$$p\text{-FC}_6\text{H}_4\text{OH} + :\text{B} \rightleftharpoons p\text{-FC}_6\text{H}_4\text{OH}\cdots:\text{B} \qquad \text{(in CCl}_4\text{)} \qquad (1)$$

No comparable relationship exists for the Kosower or Dimroth–Reichardt solvatochromic polarity scales.

EXPERIMENTAL

Solvent Purification. The liquids were dried initially for 1 week over anhydrous calcium sulfate and the esters, ethers, and
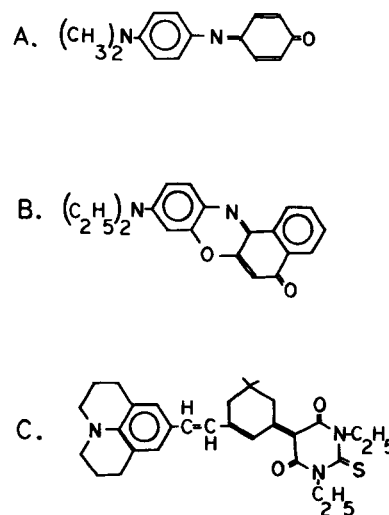

Figure 1. Structures of solvatochromic indicators investigated

(A) phenol blue (PB); (B) nile blue A oxazone (NBAO); (C) Brooker's dye VII

ketones listed in Table I were redistilled with the center two-thirds fraction being retained. All solvents were finally dried immediately prior to use by passing through a chromatographic column of activated alumina. Results from Karl Fischer titrations on the dried solvents indicated that the water contents of the liquids did not exceed 0.001%.

Solvatochromic Dyes. Phenol blue (Eastman) was purified by the two-step recrystallization and column-chromatographic resolution as described previously (7). The final product met the specifications: mp 161 °C; absorption maximum 575 nm in benzene; and single-component dye species by thin-layer chromatography (7).

The starting material for the preparation of nile blue A oxazone was commercial nile blue A sulfate (CI No. 51180, Allied Chemical), ranging in stated purity from 78 to 82%. Several attempted syntheses of the oxazone by the method of Thorpe (13) produced a product of lower mp than expected and in poor yield (less than 10%). Therefore, the method of preparation was modified as follows. One gram of nile blue A sulfate was dissolved in 125 ml of 6% (v/v) aqueous H_2SO_4 in a 500-ml round-bottom flask and 100 ml of xylene was added. The mixture was continuously stirred in a reflux arrangement while heated at 100 °C for 24 h and the crude oxazone was isolated as a residue from evaporation of the organic layer. The impure dye was then recrystallized twice from acetone–petroleum ether (1:1 v/v) followed by resolution on an alumina chromatographic column with benzene–2-propanol (1:1) as the migrating solvent. After the fluorescent red zone was well separated, the column was dismantled, and the oxazone segment was mechanically isolated and then extracted with acetone. The extract was evaporated to dryness and the residue recrystallized again from benzene–petroleum ether.

Specifications of the purified nile blue A oxazone were: mp 204–5 °C; absorption maximum in benzene 521 nm with a symmetrical peak; and homogeneous to thin-layer chromatography (Eastman Chromatogram sheet 6061) with benzene–2-propanol (1:1 v/v), R_f 0.90, and with benzene–chloroform–propanol (7). It should be noted that the crude oxazone obtained from the initial xylene layer was at least a three-component mixture based upon TLC results.

Table I. Summary of Data for Indicators in Solvents (at 25 °C)

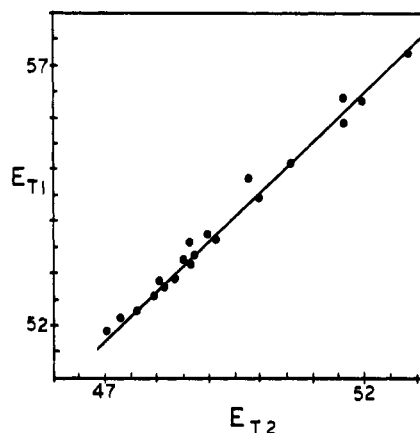| Lewis base	NBAO	PB	Brooker's dye[c]	$-\Delta G_f^0$-(PFP)[d]
		E_T for		
1 Acetone	53.64[a]	49.12[b]	45.7	1.60
2 Acetonitrile	53.74[a]	48.96[b]	45.7	1.43
3 2-Bromopyridine	57.26	52.81		1.28
4 2-Butanone			45.4	1.63
5 Cyclohexanone	53.18	48.67	44.3	1.79
6 Diethyl ether	56.39[a]	51.58	48.3	1.38
7 N,N-Dimethyl-acetamide			43.0	3.29
8 N,N-Dimethyl-formamide	52.85[a]	48.06	43.7	2.81
9 Dimethyl sulfoxide	52.17[a]	47.26[b]	42.0	3.46
10 Ethyl acetate	54.54	49.98[b]	47.2	1.49
11 Pyridine	52.55	47.98	43.9	2.56
12 Quinoline	52.65			1.78
13 Tetrahydrofuran	53.31	48.72	46.6	1.70
14 1,1,3,3-Tetra-methylurea	52.28	47.60		3.10
15 Triphenyl phosphate	52.75	48.19		2.35

[a] Values reported by Davis and Hetzer (10) and experimentally confirmed. [b] Data given by Figueras (6) and confirmed. [c] Results listed by Brooker et al. (4). [d] Values compiled by Arnett et al. (12).

Figure 2. Correlation of transition energies obtained from NBAO (E_T)$_1$ and PB (E_T)$_2$ in aprotic solvents, using data from Table I

Figure 3. General correlation of transition energies (E_T) with changing ΔG_f^0 for hydrogen bonding toward p-fluorophenol

Numbered points correspond to the bases listed in Table I. (Curve A) nile blue A oxazone; (curve B) phenol blue; (curve C) Brooker's dye VII

Spectral Methods.

Absorption spectra within the range 400–700 nm for PB and NBAO were determined in the various solvents with a Perkin-Elmer Coleman 111 spectrophotometer, using the same procedures as before (7). The values for λ_{max} were determined graphically from a minimum of five spectra with each solvent, using dye concentrations from 10^{-5} to 10^{-6} M. Transition energies listed in Table I include both new data for eight solvents and redetermined values for the remaining bases from cited literature. The uncertainties in measured λ_{max} values for the two dyes do not exceed ±0.5 nm (±0.04E_T); however, the reliability of the X_R (Brooker) energies is probably of the order of ±0.1–0.5 kcal/mol.

RESULTS AND DISCUSSION

Initially, the internal compatibility of the data for the solvent-induced red shifts obtained with the individual dyes was tested by making plots of (E_T)$_1$ vs. (E_T)$_2$ for dye pairs (1 and 2) among the three indicators studied. The graph for the case of PB–NBAO is shown in Figure 2, and data points from the published work of Davis and Hetzer (10) and Figueras (6) are included along with new experimental values from Table I. It should be noted that the two most deviant points from the line occur for benzene and chlorobenzene. The correlation coefficient for the linear function in Figure 2 is 0.993, based upon 19 aprotic solvents. Similar plots made for the other pairs, Brooker's dye VII vs. PB and Brooker's dye VII vs. NBAO, were essentially linear though less precise (14) and the regression lines yielded correlation coefficients of 0.961 and 0.958, respectively, for 17 solvents.

In their original investigation of the merocyanines Brooker et al. (4) pointed out that red-shift transition energies do not generally correlate to any significant degree with the blue-shift data obtained with alkylpyridinium iodides (Kosower) or the pyridinium betaines (Dimroth–Reichardt). This conclusion has been extended in the critical review of Fowler, Katritzky, and Rutherford with the demonstration that the Kosower and Dimroth functions exhibit a primary dependence upon the dielectric constant of the solvent and its hydrogen bond donor capacity (15). Single-parameter correlations for the blue-shift indicators
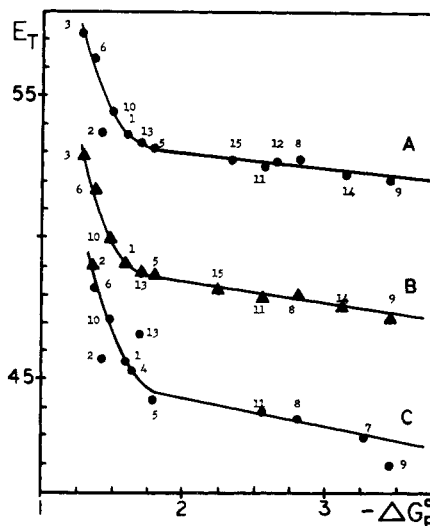
are poorest in nonpolar and polar aprotic solvents, and it follows that these dyes show little sensitivity toward changes in Lewis basicity in such media. Similarly, Krygowski and Fawcett deduced from multiple parameter comparisons that the Kosower Z values represent mainly a response of the indicator ion pair to the acidic properties of the solvent (16). By contrast, the red shift solvatochromic indicators in Figure 1 are highly sensitive to changes in Lewis basicity for polar and nonpolar aprotic media and for the lower alcohols.

Recently, an empirical mathematical model for Lewis acid–base interactions was developed by Krygowski and Fawcett in which the E_T (Dimroth) values as an acidity parameter are combined with the Gutmann donor number (enthalpy of adduct formation) for SbCl$_5$–base reactions (16). The success of their model justified the initiation of the current study of possible relationships between bathochromic E_T values as a measure of solvent basicity and thermodynamic quantities describing solvent interactions with a reference Lewis acid. For the latter, all of the ΔH, C, and E parameters in the "double-scale enthalpy equation" of Drago et al. (11), as well as the ΔH_f^0, ΔS_f^0, and ΔG_f^0 and K_f data for eq 1, were used in one- and two-parameter comparisons to E_T values from Table I. No correlations to the

enthalpy functions of Drago et al. (11), Gutmann (17), or Arnett et al. (12) were found. The same conclusion applies to the entropy changes for eq 1 as well. However, when solvatochromic red shifts (as E_T) for each of the three dyes are plotted as a function of ΔG_f^0 for the equilibrium in eq 1, the regular nonlinear correlations in Figure 3 are obtained.

Another test of the uniformity of the red-shift data for the three indicators was applied to the empirical curves in Figure 3. The parallel character of the family of curves was verfied by determining differences, $\Delta = (E_T)_2 - (E_T)_1$, for each of the solvents in Table I with a given pair of indicators (1 and 2). For the pair, NBAO–PB, the mean value of Δ (or $\bar{\Delta}$) is 4.63 ± 0.15 kcal/mol (S.D.) with all solvents included, and, for the remaining combinations, $\bar{\Delta}(PB - X_R)$ is 3.7 ± 0.9 and $\bar{\Delta}(NBAO - X_R)$ is 8.3 ± 1.0 kcal/mol. The statistical variation within a set of differences is definitely random and the poorer precision for the last two pairs arises from the larger uncertainties in the Brooker X_R data. For the more extended lower portions of the curves (beyond $-\Delta G_f^0 = 1.60$), the correlations become essentially linear and conform to a simple additivity of free energies

$$-(E_T + \Delta G_f^0) = c \qquad (2)$$

given by eq 2. The computed values for the constant, c, are: 55.20 ± 0.26 (NBAO); 50.60 ± 0.15 (PB); and 46.6 ± 0.6 (Brooker's dye VII).

LITERATURE CITED

(1) E. M. Kosower, J. Am. Chem. Soc., **80**, 3253 (1958).
(2) K. Dimroth et al., Justus Liebigs Ann. Chem., **661**, 1 (1963).
(3) C. Reichardt, Angew. Chem., Int. Ed., Engl., **4**, 29 (1965).
(4) L. G. S. Brooker et al., J. Am. Chem. Soc., **87**, 2443 (1965).
(5) J. Figueras, P. Scullard, and A. Mack, J. Org. Chem., **36**, 3497 (1971).
(6) J. Figueras, J. Am. Chem. Soc., **93**, 3255 (1971).
(7) O. Kolling and J. Goodnight, Anal. Chem., **45**, 160 (1973).
(8) O. Kolling and J. Goodnight, Anal. Chem., **46**, 482 (1974).
(9) E. G. McRae, J. Phys. Chem., **61**, 562 (1957).
(10) M. M. Davis and H. Hetzer, Anal. Chem., **38**, 451 (1966).
(11) R. Drago, G. Vogel, and T. Needham, J. Am. Chem. Soc., **93**, 6014 (1971).
(12) E. Arnett, E. Mitchell, and T. Murty, J. Am. Chem. Soc., **96**, 3875 (1974).
(13) J. F. Thorpe, J. Chem. Soc., 324 (1907).
(14) O. Kolling, Anal. Chem., **38**, 1424 (1966).
(15) F. Fowler, A. Katritzky, and R. Rutherford, J. Chem. Soc. B, 460 (1971).
(16) T. Krygowski and W. Fawcett, J. Am. Chem. Soc., **97**, 2143 (1975).
(17) V. Gutmann and R. Schmeid, Coord. Chem. Rev., **12**, 263 (1974).

Decomposition and Analysis of Refractory Oceanic Suspended Materials

D. W. Eggimann* and P. R. Betzer

Department of Marine Science, University of South Florida, 830 First Street South, St. Petersburg, Fla. 33701

A new technique for the decomposition of refractory oceanic suspended matter has been developed and tested using samples of certified standard materials, W-1 and Plastic Clay. Decomposition is carried out in a sealed, all-Teflon (T.F.E.) vessel using high-purity HCl, HNO₃, and HF. Eliminating boric acid from the digestion procedure and only using highly purified acids produces extremely low blanks, improves signal-to-noise ratios, and minimizes interferences for flameless atomic absorption analyses. Aluminum, calcium, iron, magnesium, manganese, and silicon were quantitatively recovered from standards whose weights (100 to 2000 µg) were representative of the amounts of suspended matter which would normally be filtered from open-ocean waters.

Suspended materials in open-ocean waters can vary from as little as 0.5 µg/l. to as much as 1000 µg/l. (1–6). The greatest portion of ocean waters, however, is characterized by suspended particle loads of less than 20 µg/l. (2–5). Since the largest volume water sampler which is routinely used by oceanographers collects 30 l. of seawater, the total mass of suspended material which can be collected for analysis will almost always be less than 600 µg. A large fraction (usually more than 50%) of the suspended material is made up of organic compounds; the remainder is composed mostly of alumino silicates, quartz, carbonates, and amorphous silica (1, 2, 5, 7–9).

Many of the techniques which have been applied to the decomposition and analysis of oceanic sediments (10–12)

or suspended material from rivers and other near-shore oceanic areas (13–16) are not suitable for use with samples of suspended matter collected from the open ocean because: (1) they are designed for larger sample sizes (1 mg or more of suspended matter) than are normally collected and available for analysis (10–12); (2) they use relatively large amounts of impure reagents which contribute substantial amounts of several geochemically important minor elements, including six (aluminum, calcium, iron, magnesium, manganese, and silicon) which we were interested in measuring (9–16); and (3) the samples are decomposed in open vessels which provide an avenue for atmospheric contamination and the loss of volatile species (13–18). The object of this work was to develop a suitable method for dissolving and analyzing small quantities (less than 2 mg) of oceanic suspended matter for aluminum, calcium, iron, magnesium, manganese, and silicon.

EXPERIMENTAL

The suspended material is dissolved as follows: An Eppendorf pipet is used to inject 750 µl of concentrated (ULTREX J. T. Baker Chemical Co.) HCl into an all-Teflon bomb (Figure 1) containing the suspended matter and Nuclepore filter membrane (47-mm diameter, 0.4 µm pore size) on which it was collected. The bomb is then sealed, submerged in a hot-water bath, and heated for 30 min at 90–100 °C. The bomb is then transferred to a freezer and cooled for 15 min at −45 °C. After cooling, the bomb is opened, injected with 250 µl of concentrated, ULTREX HNO₃ using an Eppendorf pipet, sealed, and submerged for an additional 30 min in the hot-water bath. Following a second cooling in the freezer, 50 µl of concentrated, ULTREX HF is injected into the bomb with an Eppendorf pipet. The bomb is then resealed and